

# *H3K36* Methylation Reprograms Gene Expression to Drive Early Gametocyte Development in *Plasmodium Falciparum*

**Jessica Connacher**

University of Pretoria

**Gabrielle A Josling**

Pennsylvania State University - Main Campus: The Pennsylvania State University - University Park Campus

**Lindsey M Orchard**

The Pennsylvania State University

**Janette Reader**

University of Pretoria

**Manuel Llinas**

The Pennsylvania State University

**Lyn-Marie Birkholtz** (✉ [lbirkholtz@up.ac.za](mailto:lbirkholtz@up.ac.za))

Department of Biochemistry, Genetics and Microbiology, Institute for Sustainable Malaria Control, University of Pretoria, Hatfield 0002, South Africa <https://orcid.org/0000-0001-5888-2905>

---

## Research

**Keywords:** H3K36me2, H3K36me3, histone, malaria, Plasmodium, gametocyte, epigenetics, histone post-translational modifications, histone demethylation

**Posted Date:** January 4th, 2021

**DOI:** <https://doi.org/10.21203/rs.3.rs-136128/v1>

**License:**   This work is licensed under a Creative Commons Attribution 4.0 International License.

[Read Full License](#)

---

**Version of Record:** A version of this preprint was published at Epigenetics & Chromatin on April 1st, 2021. See the published version at <https://doi.org/10.1186/s13072-021-00393-9>.

# Abstract

**Background:** The *Plasmodium* sexual gametocyte stages are the only transmissible form of the malaria parasite and are thus responsible for the continued transmission of the disease. Gametocytes undergo extensive functional and morphological changes from commitment to maturity, directed by an equally extensive control program. Several interconnected mechanisms governing sexual commitment have been described. However, the processes that drive the subsequent differentiation and development of the gametocyte remain largely unexplored. Using chromatin immunoprecipitation followed by high-throughput sequencing we describe an association between H3K36 di- and tri-methylation (H3K36me<sub>2&3</sub>) and the global changes in the transcriptional program driving gametocyte development post-commitment.

**Results:** Here, we show that in stage II gametocytes, H3K36me<sub>2&3</sub> are associated with an active repression of genes involved in asexual proliferation and sexual commitment, linking H3K36me<sub>2&3</sub> to the transition from early gametocyte differentiation to intermediate development. Specifically, we establish a link between H3K36me<sub>2&3</sub> and the repression of genes that are upregulated during commitment once terminal differentiation renders their protein products obsolete in developing gametocytes, thereby securing an appropriate transcriptional environment for intermediate gametocyte development. Lastly, we associate the enhanced potency of JIB-04 in gametocytes with the inhibition of H3K36me<sub>2&3</sub> demethylation and a disruption of normal transcriptional programs.

## **Conclusions:**

Taken together, our results provide the first description of an association between global gene expression reprogramming and histone post-translational modifications during *P. falciparum* sexual development. In addition to fulfilling the same role in virulence gene regulation as in asexual parasites, the stage II gametocyte-specific abundance of H3K36me<sub>2/3</sub> manifests as a largely interdependent enrichment of the two modifications targeted towards genes whose functions become obsolete in post-commitment gametocytes. This contrasts with the broad repression associated with wide-spread H3K36me<sub>2</sub> occupancy in asexual parasites, highlighting H3K36me<sub>2/3</sub> enrichment as a marker of directed transcriptional repression specific to early gametocytes. The importance of such histone methylation during gametocyte development is underscored by the transcriptional disruption associated with histone demethylase inhibition in *P. falciparum* gametocytes. By demonstrating the participation of H3K36me<sub>2&3</sub> in gametocyte development, we provide a more thorough understanding of the link between epigenetic mechanisms and gene expression in the transmissible stages of the malaria parasite.

## Background

Malaria remains a serious threat to public health in much of the developing world and is responsible for millions of deaths annually (1). Nevertheless, progress is being made toward global eradication of the

disease. Malaria eradication relies on preventing the transmission of *Plasmodium* parasites between human hosts, facilitated by the mosquito vector. In the human host, malaria parasites exist either as the asexual proliferative stages, responsible for the symptoms of malaria or as sexually differentiated, transmissible gametocytes (2, 3). The extended 10-12-day process of gametocyte development is characterised by morphologically distinct stages (I-V) and is unique to the human malaria parasite, *Plasmodium falciparum*. Mature gametocytes are the only stage that can be transmitted by the mosquito vector and as such, the process of gametocytogenesis is an attractive target for the development of transmission-blocking strategies (4–6).

The stage transitions within the *P. falciparum* parasite life cycle are driven by global transcriptomic reprogramming that is tightly controlled by complex transcriptional and post-transcriptional regulation (7–9). Additionally, epigenetic mechanisms are known to establish and maintain transcriptional programs that support asexual parasite proliferation and have been suggested to do the same during gametocytogenesis (10). The histone post-translational modification (hPTM) landscape in *P. falciparum* parasites is dynamic with each life cycle stage characterised by a unique pattern of hPTMs, suggested to be foundational in establishing the specialised transcriptional program for the stage (11). Accordingly, several hPTMs are confirmed to be functionally relevant for asexual parasite proliferation (12). For example, H3K4me3, H3K8ac and H3K9ac are involved in the activation of stage-specific gene sets that are linked to proliferation and the maintenance of the euchromatic genome that is characteristic of asexual parasites (13–17). By contrast, H3K36me2 has been proposed to be globally repressive in asexual parasites (18) and while more frequently associated with broad maintenance functions such as the conservation of genomic integrity, H3K36me2 has also been shown to direct transcriptional repression in other eukaryotes (19–21). H3K36me3 is also associated with gene silencing and controls the expression of multi-gene families that encode invasion proteins and nutrient transporters, thereby contributing to the parasite's extensive capacity for phenotypic plasticity (22–24).

During proliferation, certain gametocyte-specific genes are silenced by their association with heterochromatin protein 1 (HP1) that is recruited by an enrichment of H3K9me3 at these loci. (25, 26). Sexual differentiation involves the release of these genes from H3K9me3/HP1-mediated heterochromatin, resulting in a transcriptional environment that drives commitment to gametocytogenesis (27–30). As such, epigenetic mechanisms are known to be key factors contributing to commitment. However, only a handful of studies have examined the functional relevance of epigenetic mechanisms in post-commitment gametocyte development (26, 27, 31). Aside from the demonstrated role of H3K9me3 in initiating heterochromatin formation in late gametocytes (5), the function of hPTMs in generating and maintaining gametocyte-relevant transcriptional programs during sexual development have not been studied. The dynamic nature of the hPTM landscape during gametocyte development and departure from the patterns observed during asexual proliferation suggest that hPTMs may be involved in stage-specific gene expression in gametocytes as has been demonstrated for asexual parasites (10, 12, 16, 26, 27, 32, 33). Indeed, the concurrent shifts in the hPTM and transcriptomic landscapes associated with morphological transitions in gametocytes support this idea (11, 34). Of particular interest to us was the striking peak abundance of H3K36me2&3 unique to stage II gametocytes that corresponds to the

transcriptomic and morphological changes associated with the transition from early differentiation (stage I/II) to intermediate (stage III/IV) development (11, 34). H3K36me2&3 are both well-documented regulators of eukaryotic cellular differentiation and development (19, 35, 36) and consequently, we sought to interrogate the function relevance of these hPTMs in gametocytogenesis (11). To do so, we performed chromatin immunoprecipitation followed by high-throughput sequencing (ChIP-seq) on three distinct gametocyte populations and integrated the results with data from other ChIP-seq and gene expression profiling studies. Here we provide comprehensive genome-wide maps of the H3K36me2&3 occupancy during gametocytogenesis and show H3K36me2&3 enrichment in stage II gametocytes is associated with the transcriptional reprogramming underlying the transition from early gametocyte differentiation to intermediate development (34). Additionally, we assessed the effects of chemically inhibiting histone demethylases (HDMs) on H3K36me2&3 levels and gene expression during early gametocyte development. Using histone methylation profiling and whole transcriptome analysis, we demonstrate the link between H3K36me2&3 demethylation and the enhanced potency of the pan-selective Jumonji inhibitor, JIB-04 in gametocytes (37, 38). This paper provides the first association between H3K36me2&3 and gene regulation in gametocytes and confirms the dynamic deposition and removal of such hPTMs during *P. falciparum* sexual differentiation and development.

## Results

### H3K36me2&3 occupancy is dynamic in *P. falciparum* gametocytes

To investigate the functional role of H3K36me2&3 in *P. falciparum* stage II gametocytes (11), we performed ChIP-seq on three distinct gametocyte populations spanning early gametocyte development and classified these as “pre-stage II”, “stage II” and “post-stage II” gametocytes. Specific gametocyte populations were attained using microscopic evaluation of Giemsa-stained parasites (Additional file 1: Figure S1A) for each set of two biological replicates, which indicated that the pre-stage II samples consisted mostly of asexual parasites ( $60 \pm 4\%$ ) with some stage I ( $40 \pm 4\%$ ) and stage II gametocytes ( $0.3 \pm 0.4\%$ ) present (Fig. 1a). Stage II samples were enriched for stage II gametocytes ( $74 \pm 3.2\%$ ) with minor proportions of stage I ( $9 \pm 6\%$ ) and stage III ( $17 \pm 2.5\%$ ) gametocytes present but no asexual parasites. Post-stage II samples consisted mostly of stage III/IV gametocytes ( $90 \pm 6\%$ ) and only a small proportion ( $10 \pm 6\%$ ) of stage II gametocytes. These compositions were deemed sufficiently divergent to detect changes in H3K36me2&3 occupancy during stages I-III of gametocytogenesis and were thus used for ChIP-seq with  $\alpha$ -H3K36me2&3 antibodies that specifically detect *P. falciparum* histone H3 with the respective hPTM (either H3K36me2 or H3K36me3, Additional file 1: Figure S1B). ChIP-seq was performed using two independent biological replicates for each sample except for  $\alpha$ -H3K36me3 in pre-stage II gametocytes which had only one. Data for corresponding replicate samples were well correlated (e.g., Pearson correlation,  $r^2 = 0.73$ ,  $r^2 = 0.93$  and  $r^2 = 0.94$  for H3K36me2 in pre-stage II, stage II and post-stage II samples, respectively, Additional file 2: Table S1). We detected H3K36me2 and H3K36me3 individually in each of the sampled gametocyte populations and observed a strong positive correlation between the presence of these two hPTMs in the stage II gametocytes (Pearson correlation,  $r^2 = 0.9$ ). Given that a

single nucleosome would not contain di- and trimethylated H3K36 concurrently, this likely reflects that one of these hPTMs is an intermediate in the formation of the other with our samples consisting of a combined pool of nucleosomes with either state of methylation. Such robust correlations between H3K36me2&3 were absent for the pre- and post-stage II gametocytes with each of these samples additionally not correlated with the stage II samples (e.g. for correlations between pre-stage II and stage II gametocytes,  $r^2 = -0.46$  for H3K36me2 and  $r^2 = 0.06$  for H3K36me3, Fig. 1b, Additional file 1: Figure S1C).

Our ChIP-seq results show that unique patterns of H3K36me2&3 occupancy occur at each of the gametocyte stages and that both hPTMs are differentially enriched in the stage II gametocytes (Fig. 1c). The presence of H3K36me2&3 is dynamic with patterns of “low-high-low” hPTM abundance associated with pre-stage II, stage II and post-stage II gametocyte populations, respectively. These stage-specific occupancy profiles were confirmed independently by ChIP-qPCR (Additional file 1: Figure S2). Consistent with the stage-specific enrichment dynamics reported previously for *P. falciparum* H3K36me2&3, these results validate the experimental strategy used to detect changes in the hPTM landscape during gametocyte development. As highlighted in a central region of chromosome 12 (1250–1290 kb), both H3K36me2&3 were detected at low levels in pre-stage II gametocytes. However, this contrasts sharply with an abundance of both hPTMs in the stage II gametocytes in which the enrichment was preferentially intergenic and upstream of the coding regions of genes. In post-stage II gametocytes, the levels of the hPTMs dissipate, as evidenced by residual H3K36me2&3 occupancy at sites that were highly enriched in the preceding stage II gametocyte samples (Fig. 1c). Given the unique abundance of H3K36me2&3 in the stage II gametocytes and the congruency of this with our previous proteomics data, our downstream analyses focussed on the preferential enrichment of these hPTMs upstream of genes in the stage II gametocytes.

## Stage II gametocytes have a unique pattern of H3K36me2&3 enrichment upstream of genes

To determine the genome-wide positioning of H3K36me2&3, we interrogated the hPTM occupancy spanning each of *P. falciparum* genes for which sequencing data were obtained (5602 genes, Additional file 2: Table S2, Fig. 2a). The occupancy profiles of H3K36me2&3 are distinctly uniform across the intergenic non-coding regions in stage II gametocytes, contrasting with more variable patterns in the pre- and post-stage II gametocytes (Fig. 2a). In stage II gametocytes, both H3K36me2&3 are concentrated 750 bp upstream of gene start sites (SS) with average occupancies ( $\log_2$ ChIP/input) over this region of 0.2 and 0.15 (peaking at 0.24 and 0.2) for H3K36me2&3, respectively, with a contrasting lack of enrichment ( $\log_2$ ChIP/input < 0.2 and < 0.15 for H3K36me2&3, respectively) or complete depletion ( $\log_2$ ChIP/input  $\leq 0$ ) in coding regions (Fig. 2a). In the pre- and post-stage II gametocytes, both hPTMs are on average depleted 750 bp upstream of the gene SS (e.g. average H3K36me2 occupancy of -0.14 and -0.001 over this region in pre- and post-stage II gametocytes, respectively), emphasising the prominent abundance of H3K36me2&3 upstream of genes that is exclusive to the stage II gametocytes.

Next, we quantified the number of genes for which H3K36me2/3 occupancy was detected and stratified this according to location (Fig. 2b). In stage II gametocytes, H3K36me2&3 were detected upstream of 89% (4969) and 83% (4677) of genes occupied ( $\log_2\text{ChIP}/\text{input} > 0$ ) by either of these modifications, respectively (Fig. 2b). Of these, 3942 and 3776 genes had occupancy exclusive to the upstream regions while only a minor proportion (85 and 75) of the genes had H3K36me2&3 exclusively present in the coding regions, respectively (Additional file 1: Figure S3A). This contrasts sharply with the distribution of the hPTMs in pre- and post-stage II gametocytes, where coding region occupancy is evident (Fig. 2b, Additional file 1: Figure S3B). In post-stage II gametocytes, both H3K36me2&3 were distributed relatively equally across the upstream and coding regions of genes (Fig. 2b). Unexpectedly, low level H3K36me2 occupancy (average  $\log_2\text{ChIP}/\text{input} = 0.07$ ) was pervasive in the coding regions of pre-stage II gametocytes (4292 genes, Additional file 1: Figure S3A). Since the pre-stage II gametocyte samples used for ChIP-seq still contained a relatively large subpopulation of asexual parasites, this occupancy likely results from the detection of H3K36me2 in these stages where coding region occupancy has been reported to be linked to gene repression (18, 22).

The wide-spread occupancy patterns of H3K36me2&3 in stage II gametocytes each translate to a large number of genes where the hPTMs are enriched (Fig. 2c). For H3K36me2, 2480 genes were enriched with the hPTM 750 bp upstream of the SS and a further 226 genes were robustly enriched ( $\log_2\text{ChIP}/\text{input} \geq 0.5$ ). Although also detected in the coding regions of 23% of genes (599) with upstream enrichment, only four of these had H3K36me2 enrichment extending to their coding region (Additional file 1: Figure S3C). Similarly, H3K36me3 was enriched upstream of 2691 genes in stage II gametocytes with 85 of these exhibiting robust enrichment (Fig. 2c). Approximately 25% of these enriched genes also had H3K36me3 associated with the coding regions however, only 15 were enriched for the hPTM in this region (Additional file 1: Figure S3C). Taken together, these results indicate that H3K36me2&3 occupancy occurs in a pattern unique to and characteristic of stage II gametocytes. Furthermore, a concentration of the hPTMs upstream of gene SS, where they would be ideally situated to influence expression by virtue of their proximity to promoters, suggests functional roles for H3K36me2&3, exclusive to stage II gametocytes.

### **Enrichment of H3K36me2&3 upstream of genes is associated with reduced transcript levels in stage II gametocytes**

To explore the functional roles of H3K36me2&3 in stage II gametocytes, we compared the levels of hTPM occupancy upstream of gene SS with expression levels from a publicly available gene expression time course data set (34). Corresponding expression profiles were obtained for days 2–6 of gametocyte development (days on which stage II gametocytes were present) for 96% and 95% (2594 and 2545 genes) of the H3K36me2&3-enriched genes, respectively (Additional file 2: Table S3). The global analysis of the hPTMs upstream of genes and the transcript levels in stage II gametocytes (average  $\log_2\text{Cy5}/\text{Cy3}$  on days 4 and 5 of development associated with stage II gametocytes) indicated that the degree of H3K36me2&3 occupancy is not correlated with the expression (Pearson correlations,  $r^2 = -0.12$  and  $r^2 = -0.1$  for H3K36me2&3, respectively, Fig. 3). The contrasting depletion of H3K36me2&3 upstream of genes

in the other stages, particularly in pre-stage II gametocytes (Additional file 1: Figure S4A), implies that in the stage II gametocytes, these hPTMs are associated with an active repression of genes that are not required for gametocyte development. Indeed, 63% of these H3K36me<sub>2/3</sub>-enriched and repressed genes (Additional file 2: Table S3) have been shown to be indispensable for asexual proliferation previously (39). This is furthermore supported by the increasing anti-correlation ( $r^2 = -0.026$  and  $-0.02$  on day 2 and  $r^2 = -0.13$  and  $-0.14$  on day 6 for H3K36me<sub>2&3</sub>, respectively, Additional file 1: Figure S4A) between hPTM abundance and transcript levels for the enriched genes in stage II gametocytes. Additionally, for genes without H3K36me<sub>2/3</sub> enrichment, this relationship was weakened or reversed (corresponding  $r^2 = 0.02$  and  $0.03$  on day 2 and  $r^2 = -0.03$  and  $-0.01$  on day 6). The H3K36me<sub>2</sub>-enriched genes clustered into three groups based on expression profiles (Fig. 3a) with ~98% (2548 genes) of the genes showing reduced transcript abundance. A similar pattern was present for H3K36me<sub>3</sub> with ~98% (2545 genes) of the genes enriched for this hPTM repressed in the stage II gametocytes (Fig. 3b). The H3K36me<sub>2&3</sub>-enriched repressed gene sets are significantly ( $P$ -value < 0.05) associated with shared and unique biological processes (Fig. 3), reflecting the large proportion of genes in the stage II gametocytes that were enriched for both H3K36me<sub>2&3</sub> (2012 genes, i.e. 80%), Additional file 1: Figure S4B, Additional file 2: Table S3) and 20% of each set uniquely enriched (695 and 680 genes for H3K36me<sub>2&3</sub>, respectively). This overlap suggests that one of the H3K36 methylation states is a transient intermediate in the generation of the other (22).

The biological processes associated with genes enriched for H3K36me<sub>2&3</sub> include those that are well established to be essential in the proliferative parasite stages (e.g. signal transduction, antigenic variation, gene expression and DNA replication) and include genes coding for Maurer's cleft proteins (e.g. *rex1*, PF3D7\_0935900 and *rex4*, PF3D7\_0936400) members belonging to the major invasion families (e.g. *rhs*, *ebas*, *vars*, *rifs* and *msps*) and components of the cytoadherence complex (e.g. *kahsp40*, PF3D7\_0201800 and *kahrp*, PF3D7\_0202000, Fig. 3, Additional file 2: Table S4) (34, 39, 40). Similar to the role previously ascribed to H3K36me<sub>3</sub> as a repressor of invasion gene families when associated with regions upstream of genes in asexual parasites (18, 22), we find the majority of the erythrocyte membrane proteins (*emp1s*, 75%), *stevors* (94%) and *rifins* (70%) are enriched for H3K36me<sub>3</sub> in stage II gametocytes, suggesting the control of variant gene expression by H3K36me<sub>3</sub> is not limited to asexual parasites but is conserved across multiple life cycle stages. Additionally, most of these genes are also enriched for H3K36me<sub>2</sub> as an intermediate, as in the asexual stages (22). Interestingly, within the process of chromatin remodelling, all four *P. falciparum* histone acetyltransferase (HAT) -encoding genes (14, 41) that generate transcriptionally active chromatin structures (17, 19) were enriched and repressed by H3K36me<sub>2&3</sub>. Various processes that have been documented to be functionally important during sexual commitment and early gametocyte differentiation including chromatin remodelling ( $P = 0.04$ ), protein translocation ( $P = 0.01$ ) and phosphatidylcholine (PC) biosynthesis ( $P = 0.003$ ) (27, 29, 42–46) are significantly associated with the H3K36me<sub>2&3</sub>-enriched gene sets (Fig. 3). Interestingly, the only processes where H3K36me<sub>2&3</sub> enrichment was not associated with a definitive reduction in transcript abundance were actin filament capping, acetyl-CoA biosynthesis and intracellular signalling. Overall, these results indicate that H3K36me<sub>2&3</sub> are associated with an active repression of genes that encode

protein products involved in proliferation and sexual commitment when they become irrelevant in the developing gametocyte.

**In stage II gametocytes, H3K36me2&3 are associated with transcriptional repression of genes that are activated during sexual commitment.**

Next, we sought to further investigate the relationship between H3K36me2&3 enrichment in stage II gametocytes and transcriptional repression of commitment- and differentiation-related genes. Of a panel of 1500 sexual development-related genes compiled from previous studies (25, 27, 29, 34, 42–46), we find 64% are enriched for H3K36me2&3 in stage II gametocytes (Additional file 2: Table S5). Importantly, all the enriched genes have dramatically reduced transcript abundance levels during early gametocyte development compared to those without H3K36me2&3 (average of 6-fold and  $\leq$  12-fold lower on days 3–7, Fig. 4a). The H3K36me2&3-enriched set includes genes encoding the phosphoethanolamine methyltransferase (PMT) and ethanolamine kinase (EK) that are involved in the synthesis of PC from an alternative substrate under lysophosphatidylcholine (lysoPC) limited conditions (42, 46–49). Additionally, H3K36me2&3 enrichment is evident for genes encoding the chromatin modifying enzymes SNF2L, ISWI, the histone deacetylases HDA1 and HDA2 and the NAD<sup>+</sup>-dependent deacetylase, SIR2A, the latter of which is known to be repressed during early development and thereby blocks proliferative processes (50). Interestingly, we identify H3K36me2&3 enrichment for two histone methyltransferase (HMT) -encoding genes, *set3* (PF3D7\_0827800) and *set9* (PF3D7\_0508100). Although the targets of SET9-mediated histone methylation remain unclear, SET3 is known to di- and tri-methylate H3K9 (23, 51); H3K9me3 is well established as a repressive hPTM (16, 25, 27). Moreover, H3K36me2&3 are enriched upstream of the gene encoding Jumonji-C domain-containing protein 2 (JMJC2), a putative *P. falciparum* HDM containing the Jumonji-C domain (52) that is present in histone lysine demethylase 4 (KDM-4)/JMJC2 HDMs that demethylate di- and tri-methylated H3K9 and H3K36 in other organisms (53–55).

In addition to the above, the *ap2-g* (PF3D7\_1222600) locus was enriched for H3K36me2&3 in stage II gametocytes. AP2-G, a member of the ApiAP2 DNA-binding protein family, has been shown to be a master regulator of sexual commitment in *P. falciparum*, *P. yoelii* and *P. berghei* (28, 30, 39, 56, 57). Here we find some differentiation in the distribution of H3K36me2 vs. -me3 upstream of *ap2-g* with the former somewhat less defined in this region (Fig. 4b). Furthermore, similar H3K36me2/3 enrichment was present upstream of 67% of the genes (average upstream occupancy of 0.3 and 0.24 respectively, Fig. 4b, Additional file 1: Figure S5A) directly targeted by the AP2-G transcription factor during commitment and subsequent development (29, 58). As before, the H3K36me2&3 enrichment at the AP2-G target genes is associated with their transcriptional repression, contrasting with the expression patterns of those without enrichment (Fig. 4b). In the pre-stage II gametocytes, these AP2-G binding sites are generally depleted of H3K36me2&3 (average upstream occupancy of -0.18 and -0.3, respectively, Additional file 1: Figure S5A), including the *ap2-g* locus itself with < 1% of the target genes associated with H3K36me2/3 enrichment in this stage (Additional file 1: Figure S5B). This shows that H3K36me2&3 are involved in the active repression of genes once the protein products are no longer required following the establishment of gametocytogenesis. Similarly, in the post-stage II gametocytes, these AP2-G binding sites are generally

associated with an absence of H3K36me2&3 (average occupancy of  $4.2e^{-4}$  and  $1.8e^{-3}$ , respectively, Additional file 1: Figure S5A) with < 7% of these genes exhibiting residual H3K36me2/3 enrichment from the preceding stage II gametocytes. This is associated with a gradual increase in transcript abundance, indicating that these genes are no longer actively repressed once depleted of H3K36me2&3 enrichment in the post-stage II gametocytes (Additional file 1: Figure S5C). Although the targets of AP2-G vary between gametocytes arising from the same-cycle conversion (SCC) and next-cycle conversion (NCC) pathways (29), we find no considerable differences in the proportion of SCC and NCC AP2-G target genes that are enriched for H3K36me2&3 in stage II gametocytes (Additional file 1: Figure S5D), suggesting that the H3K36me2&3-associated transcriptional repression occurs post-commitment irrespective of the route taken during sexual differentiation.

We also assessed the H3K36me2/3 enrichment in our gametocyte populations at sites occupied by a second ApiAP2 transcription factor, AP2-G2 (PF3D7\_1408200), during intermediate gametocyte development (59). AP2-G2 is not essential for asexual parasite proliferation or sexual commitment however, the genetic disruption of *ap2-g2* stalls normal gametocyte development beyond stage III (39, 59). In pre-stage II gametocytes, 3% of the upstream AP2-G2 binding sites were enriched with H3K36me2/3. This increases drastically in stage II gametocytes where 92% of these sites are now enriched with H3K36me2/3 (Fig. 4c). This suggests an interaction between these two regulatory mechanisms and supports previous descriptions of AP2-G2 as a transcriptional repressor (59). The number of H3K36me2&3-enriched sites is somewhat reduced in the post-stage II gametocytes (54%) as expected given the residual hPTM occupancy patterns in these later gametocyte stages that are reminiscent of H3K36me2/3 enrichment in the stage II gametocytes. For AP2-G2 binding sites present in coding regions, 0.3% have H3K36me2/3 enrichment in the stage II gametocytes (Fig. 4c) and in the pre- and post-stage II gametocytes, this increases slightly to 7.5% and 11%, respectively. This implies the potential interaction of H3K36me2&3 with AP2-G2 occurs predominantly in regions upstream of genes with the enrichment of these hPTMs at these locations suggesting a stage-specific role for this interaction.

Lastly, we compared H3K36me2&3 with other epigenetic mechanisms that function in *P. falciparum* sexual commitment and development or have been implicated in gene repression and chromatin remodelling (16, 25, 27, 60, 61). The interaction between H3K9me3 and histone protein 1 (HP1) mediates global heterochromatin formation during gametocyte development in addition to its role in regulating commitment (27, 33). We find that of the 89 genes preferentially occupied by HP1 in stage II/III gametocytes relative to schizonts (27), 88% are enriched for H3K36me2&3 in stage II gametocytes, resulting in diminished transcript abundance (average of 1.5-fold and  $\geq 2.6$ -fold lower on day 3–7 compared to those without H3K36me2&3, Fig. 4d). This implies some degree of co-operativity exists between the repressive actions of H3K36me2&3 and H3K9me3/HP1 binding. Interestingly, each of the 15 genes with reduced HP1 occupancy (27) were also enriched for H3K36me2&3 in stage II gametocytes (Fig. 4d) with the presence of the two hPTMs overlapping with residual HP1 occupancy upstream of gene SS (Additional file 1: Figure S5E) These genes, including *ap2-g* and the early gametocyte markers

PF3D7\_1476500, PF3D7\_1476600, PFD7\_1477300 (*Pfg14\_744*), PF3D7\_1477400, PF3D7\_1477700 (*Pfg14\_748*) and PF3D7\_1478000 (*gexp17*) (43, 44, 62, 63), exhibit peak transcript abundance during commitment and early differentiation (days 1 and 3) followed by a steady decline in expression levels associated with the enrichment of these genes with H3K36me2&3 in the stage II gametocytes (Fig. 4d). This finding, together with the documented absence of H3K9me3 at these sites in late (stage IV/V) gametocytes (33), suggests that although the identities of the H3K36me2&3 reader protein/s remain unclear, these hPTMs are also involved in the repression of transcription independent of the H3K9me3/HP1 mechanism during gametocyte development. Interestingly, for genes that do gain H3K9me3 occupancy in late-stage gametocytes, 82% were enriched for H3K36me2&3 in stage II gametocytes (Fig. 4e). Once again, the H3K36me2&3-enriched gene set had substantially lower transcript levels compared to those without such enrichment, supporting the idea of co-operative functioning of H3K9 and H3K36 tri-methylation in *P. falciparum* gametocytes. Together, these results indicate that H3K36me2&3 are involved in generating a post-commitment transcriptional shift to allow differentiated gametocytes to continue through development.

### **Inhibition of H3K36 demethylation by JIB-04 is associated with altered patterns of transcription in *P. falciparum* gametocytes**

Lastly, we investigated the potential enzymes that generate the unique stage II gametocyte-specific enrichment of H3K36me2&3 described here and previously (11). In asexual parasites, SET2 (PF3D7\_1322100) methylates H3K36 (52, 64). The transcript levels of this HMT increase on day 1 of gametocytogenesis and subsequently decline thereafter (Fig. 5a), suggesting that the H3K36-specific methyltransferase activity of SET2 is extended to the gametocyte stages. The transcript levels of the three Jumonji KDMs of *P. falciparum* (*jmjc1* (PF3D7\_0809900), *jmjc2* (PF3D7\_0602800) and *jmj3* (PF3D7\_1122200)) spanning stage II gametocyte development strongly suggests that at least one of these enzymes is likely involved in H3K36 demethylation (Fig. 5a). To investigate the functional relevance of these enzymes for H3K36me2&3, we chemically interrogated HDM activity and determined the effects of this inhibition on H3K36 methylation levels on days associated with stage II gametocyte development. Jumonji HDM inhibitors with activity against gametocytes (38, 65, 66). JIB-04 (pan-selective) and ML324 (targeting KDM4, *PfJMJ3*) resulted in the hypermethylation of both H3K36me2&3 relative to the untreated controls (36- to 89-fold, Fig. 5b, Figure S6A), similar to hypermethylation of H3K4me3 and H3K9me3 induced by JIB-04 and ML324 in asexual parasites and gametocytes, respectively (38, 66). This hypermethylation was not observed for GSK-J4 (KDM6, H3K27me3 selective, (67) or PCPA-2 (targeting LSD1). These results confirm that at least one of the *P. falciparum* Jumonji HDMs demethylate H3K36me2&3 after they peak in abundance in stage II gametocytes (11). Furthermore, mechanistic studies in asexual parasites have demonstrated that the inhibition of demethylase activity by JIB-04 arises from the direct targeting of *PfJMJ3* (38). In the asexual parasites, the inhibition of *PfJMJ3* by JIB-04 results in transcriptional de-regulation (38). Since this inhibitor is significantly more potent towards the sexual stages (38, 66), we were particularly interested in the transcriptional effects of JIB-04 in gametocytes since this inhibitor is significantly more active against the sexual stages. As such, we performed genome-wide transcriptional profiling of JIB-04 activity on day 3 and 4 gametocytes each

following 24 h treatment with JIB-04 (Additional file 3: Table S6). JIB-04-treated gametocytes displayed differential expression of ~ 13% of the genome (711 and 696 genes with decreased and increased transcript abundance, respectively, Fig. 5c, Additional file 1: Figure S6B), similar to the restricted effect induced by this inhibitor in asexual parasites (38). Differentially expressed genes with decreased transcript abundance are associated with various processes including chromatin organisation (3%), gene expression (12%) and transport (6%), each of which have confirmed roles in gametocyte differentiation and development (27, 34, 43, 45, 46, 63, 68–70) (Fig. 5c). Of these genes, 63% were enriched for H3K36me<sub>2&3</sub> (93% with occupancy) in stage II gametocytes including the invasion-related gene families (Fig. 5c) whose post-commitment transcriptional repression we show to be associated with these hPTMs. A large proportion (93%) of the differentially expressed genes with increased abundance also had some degree of H3K36me<sub>2/3</sub> occupancy with 56% enriched for the hPTMs in the stage II gametocytes. Genes functionally associated with cellular proliferation that were enriched for H3K36me<sub>2&3</sub> in stage II gametocytes and repressed as a result, also had increased transcript abundance in response to JIB-04 treatment (Fig. 5c). Interestingly, we also find an increase in the transcript levels of *jmjc2* and the HAT-encoding genes, *gcn5* (PF3D7\_0823300) and *myst* (PF3D7\_1118600) (Fig. 5c) (14, 41), all of which may reflect an attempt to counteract the abnormal H3K36me<sub>2&3</sub>-associated repression induced by JIB-04. Combined with the depletion of H3K36me<sub>2&3</sub> beyond stage II gametocyte development, these results suggest that aberrant H3K36 hypermethylation poses a barrier to further development and highlight the importance of histone methylation for transcriptional reprogramming during gametocyte differentiation and development. Shared disruption of certain biological processes, including chromatin organisation, cell motility and kinase/phosphatase activity (38) was present (Fig. 5d). The JIB-04 treated gametocytes do not share common differentially expressed genes with the G9a methyltransferase specific inhibitors, BIX-01294 (71) but some overlap is present with HDAC inhibition by Trichostatin A (72), in line with other studies which showed similarities in the gene expression signatures of JIB-04 and TSA in cancer cell lines (73).

## Discussion

Understanding the gene regulatory mechanisms that drive differentiation and development in *P. falciparum* gametocytes is essential for the discovery and advancement of novel malaria transmission-blocking strategies (74). Here, we confirmed the dynamic yet stage-specific nature of H3K36me<sub>2&3</sub> (11) and delineate their roles in the transcriptional reprogramming occurring post-commitment in the gametocyte sexual stage of *P. falciparum* blood-stage development (34). Our chemical interrogation of *P. falciparum* HDMs supports these conclusions, highlights the importance of the dynamics of histone methylation for transcriptional control and links aberrant H3K36me<sub>2&3</sub> patterns with the increased potency of Jumonji HDM inhibitors towards gametocytes reported before (38, 65, 66).

Our experimental strategy entailed the prior validation of antibody specificities for di- and tri-methylated *P. falciparum* H3K36. This was crucial as *Plasmodium*-specific antibodies were not available and the use of antibodies generated against H3K36me<sub>2&3</sub> from other organisms have yielded variable results in *P. falciparum* parasites (22, 32, 64, 75). Confirmation of the specificity of the selected antibodies provided

evidence that our ChIP-seq data accurately reflects the status of H3K36me<sub>2&3</sub> in *P. falciparum* gametocytes. Although the focus of this paper is H3K36me<sub>2&3</sub> enrichment in the stage II gametocytes, it is important to highlight that despite their comparatively lower levels of occupancy, both H3K36me<sub>2&3</sub> were detected in pre- and post-stage II gametocytes and as such we do not exclude the possibility of these hPTMs being functionally relevant in other gametocyte stages.

Our approach allowed for the delineation of genomic regions dynamically occupied by H3K36me<sub>2&3</sub> during gametocytogenesis and demonstrate that their stage II gametocyte-specific abundance (11) manifests as wide-spread, yet largely intergenic, enrichment that is congruent with the characteristic patterns of these hPTMs when functioning repressively in other organisms, particularly during cellular differentiation (76–84). In line with this, we show that H3K36me<sub>2&3</sub> enrichment in stage II gametocytes is associated with an active repression of transcription. In other eukaryotes, H3K36me<sub>2&3</sub> coding region occupancy similar to our observations in pre- and post-stage II gametocytes, is indicative of transcriptionally permissive genes (22, 85, 86). This also aligns with findings from other studies which show that in asexual parasites, SET2-mediated deposition of H3K36me<sub>3</sub> is associated with the coding region of the active *var* gene while enrichment of the hPTM upstream of silenced *var* genes is directly involved in their repression (22, 64). These similar patterns of H3K36me<sub>2&3</sub>-associated transcriptional repression in stage II gametocytes and the increased transcript levels of SET2 during early development (34), suggests this HMT is the most likely candidate enzyme of H3K36 methylation in gametocytes. In addition to the likelihood of a shared H3K36 HMT, the similarities in the MOA of JIB-04 in gametocytes and that described elsewhere for asexual parasites (38), suggests a common enzyme demethylates H3K36 in the asexual and sexual life cycle stages.

SET2-generated H3K36me<sub>3</sub> mediates transcriptional repression via the recruitment of histone deacetylases (HDACs), thereby antagonising the HAT activity that initiates transcription (17, 19, 87). We find that H3K36me<sub>2&3</sub> are involved in the repression of all four *P. falciparum* HATs (17, 41) including a robust enrichment of the gene encoding the H3-specific HAT, GCN5 (14). Furthermore, two *hdac* genes, encoding HDA1 and HDA2, both with commitment-specific roles (88, 89), are enriched for H3K36me<sub>2&3</sub>, suggesting that in *Plasmodium* parasites, these hPTMs contribute to transcriptional repression by preventing the accumulation of acetylated histones (19, 87).

Accumulating evidence demonstrates that such epigenetic regulators are essential drivers of the transcriptional reprogramming necessary for cellular differentiation (76, 90–92). Accordingly, for *P. falciparum* gametocyte differentiation, the role of hPTMs in governing the transcriptional shifts that coincide with morphological stage transitions was previously alluded to (11, 34). Here, we confirm that the stage II gametocyte-specific H3K36me<sub>2&3</sub> abundance does indeed correspond to the enrichment and repression of a large proportion of commitment-related genes during the transition from early differentiation to intermediate gametocyte development (11, 34). Specifically, the enrichment of genes that are upregulated under conditions of lysoPC depletion link H3K36me<sub>2&3</sub> with the parasite's earliest responses to the environmental cue for sexual commitment (42). The H3K36me<sub>2&3</sub>-associated repression of the *ap2-g* transcription factor (28) and chromatin modifiers (42, 88, 89) that are upregulated

and drive commitment following this cue, attest to the influential role of H3K36me<sub>2&3</sub> at this transition point. Correspondingly, H3K36me<sub>2</sub> has been shown to influence expression cascades by modulating the transcription of master regulatory factors in other organisms (76).

Post-commitment, the stage I gametocytes are morphologically and metabolically similar to the rapidly proliferating trophozoites, undergoing RNA and protein synthesis (63, 93, 94). During this phase, gametocytes remodel the deformability and adhesive properties of their host erythrocytes in preparation for the new microenvironment in the bone marrow (68, 95–97). This adaptation is supported by the continued digestion of haemoglobin, gene expression and an increase in protein export (63, 98). Thereafter, these processes are suppressed by H3K36me<sub>2&3</sub> in the stage II gametocytes, demonstrating that this point represents a key transition at which H3K36me<sub>2&3</sub> assist in generating a transcriptional environment that supports further gametocyte development.

We also find that H3K36me<sub>2&3</sub> is closely linked to both the loss and formation of heterochromatin in gametocytes in accordance with similar observations in other organisms (78, 99, 100). Firstly, the H3K36me<sub>2&3</sub> enrichment of genes that are released from H3K9me<sub>3</sub>/HP1-mediated heterochromatin during commitment and early differentiation (27) suggest these hPTMs antagonise the resulting transcriptional activation once it becomes obsolete in terminally differentiated gametocytes. Next, genes that associate with both HP1 and H3K36me<sub>2&3</sub> in early gametocytes have substantially lower transcript levels compared to those only occupied by HP1 indicating the cooperativity between these mechanisms that has been described elsewhere (78, 99, 100) is also present in *P. falciparum* parasites. Lastly, heterochromatic genes associated with H3K9me<sub>3</sub> in late gametocytes (33) are also enriched for H3K36me<sub>2&3</sub> in stage II gametocytes, supporting the link between tri-methylated H3K9 and H3K36 in heterochromatin formation. Accordingly, we show that the JMJC2-specific HDM inhibitor, ML324 leads to the hypermethylation of H3K36, in addition to the previously documented hypermethylation of H3K9 that is associated with increased potency of ML324 in late gametocytes (38, 66).

## Conclusions

This work highlights the crucial nature of the epigenetic mechanisms underlying the vast transcriptional reprogramming associated with *P. falciparum* gametocyte differentiation (11, 27, 33, 34). Here, we demonstrated an early gametocyte-specific association between H3K36me<sub>2&3</sub> and gene expression during the transition from early differentiation to intermediate development. We showed that H3K36me<sub>2&3</sub> function both independently, in concert and antagonistically with other regulatory mechanisms, including H3K9me<sub>3</sub>/HP1, AP2-G2 and AP2-G, in post-commitment gametocytes. This study reveals the functional association between H3K36me<sub>2&3</sub> and gene regulation extends beyond virulence gene families and broad general repression in asexual parasites and encompasses a gametocyte-specific link between these hPTMs and transcriptional regulation. The transcriptional remodelling that occurs during gametocyte commitment and subsequent development necessitate the existence of control mechanisms that direct these broad shifts. We propose that H3K36me<sub>2&3</sub> are important for the repression of proliferation- and commitment-specific transcripts once they become obsolete in terminally

differentiated gametocytes and thus allow for the transition into intermediate gametocyte development. Epigenetic regulatory mechanisms have been heralded as important chemotherapeutic targets for many diseases including malaria (16, 101, 102). As such, an understanding of these processes in *Plasmodium* parasites, particularly in the transmissible gametocyte stages, paves the way for the development of much-needed novel diagnostic, treatment and transmission-blocking strategies for malaria (74, 103). The findings of this study make substantial contributions to the understanding of epigenetics in *P. falciparum* gametocytes which until recently had remained largely unexplored.

## Methods

### Parasite culturing

*P. falciparum* NF54 asexual parasite cultures were maintained *in vitro* at 37 °C in human erythrocytes at a 5% haematocrit (ethics approval obtained from the University of Pretoria Research Ethics Committee, Health Sciences Faculty 506/2018) and synchronised using 5% D-sorbitol as previously described (104, 105). *P. falciparum* gametocytes were induced as previously described (106–108) through a combination of nutrient starvation and a drop in haematocrit from synchronous ( $\geq 95\%$  ring stages) asexual parasite cultures (0.5% parasitaemia, 6% haematocrit). Media (RPMI-1640, 23.8 mM Na<sub>2</sub>CO<sub>3</sub>, 0.024 mg/ml gentamycin, 25 mM HEPES, 0.2 mM hypoxanthine and 0.5% (w/v) Albumax II) was replaced 48 h after initiation. The haematocrit was reduced to 4% 72 h after initiation (hereafter referred to as day 0) and maintained as such throughout gametocyte development with daily replacement of glucose-enriched (20 mM) media. Residual asexual parasites were removed by supplementing glucose-enriched media with 50 mM *N*-acetylglucosamine (Sigma-Aldrich) from day 1 of development. Gametocytes were sampled on days 2, 4 and 7 post-induction as the pre-stage II, stage II and post-stage II samples, respectively. Two independent cultures were used as biological replicates for each ChIP-seq and ChIP-qPCR experiment. Parasite proliferation and gametocyte differentiation were monitored daily by microscopic evaluation of Giemsa-stained smears.

**Antibody validation:** The specificity of commercially obtained ChIP-grade rabbit anti-H3K36me<sub>2</sub> (Abcam, ab9049) and anti-H3K36me<sub>3</sub> (Abcam, ab9050) antibodies was tested using modified and unmodified synthetic peptides (Genscript) of the *P. falciparum* 3D7 histone H3 sequence (Additional file 4: Table S7. Modified peptides were di- or tri-methylated on K9 or K36 each with a corresponding unmodified K9 (ARTKQTARKSTAGKAPRKQ) and K36 (ARKSAPISAGIKKPHRYRPG) peptide. Nitrocellulose membranes spotted with 25 ng of each peptide were blocked for 30 min in blocking buffer (5% milk powder in TBS-t (50 mM Tris (pH 7.5), 150 mM NaCl and 0.1% (v/v) tween-20) and incubated with primary antibodies (1:5000) against H3K36me<sub>2</sub> or H3K36me<sub>3</sub> overnight followed 1 hr incubation with secondary antibody (1:10000 goat anti-rabbit IgG conjugated to HRP). Chemiluminescent signal (Pierce Super Signal West Pico PLUS Chemiluminescent Substrate) was quantified by densitometry using ImageJ analysis software (109).

**Chromatin immunoprecipitation:** ChIP was performed as previously described (29) with modifications. Gametocytes (1–3% gametocytaemia, fixed in 1% formaldehyde for 10 min at 37 °C followed by 0.125 mM glycine quenching) were released from erythrocytes using 0.1% (w/v) saponin. Thereafter, the gametocytes were resuspended in lysis buffer (10 mM Hepes (pH 7.9), 10 mM KCl, 0.1 mM EDTA (pH 8.0), 0.1 mM EGTA (pH 8.0)) and lysed with 0.25% Nonidet P-40 and douncing. Nuclei were then resuspended in Covaris shearing buffer (0.1% sodium dodecyl sulfate (SDS), 10 mM Tris (pH 8.1), 1 mM EDTA) and sonicated with the conditions: 5% duty cycle, 75 W peak incident power, 200 cycles per burst for a total treatment time of 300 s using a M220 ultrasonicator (Covaris). The sonicated chromatin was then pre-cleared using Protein A/G magnetic beads (Millipore 16–663) and aside from a small quantity kept separately as input material, chromatin was incubated overnight with 3 µg of anti-H3K36me2 or anti-H3K36me3. Reversal of cross-linking was achieved by adding 0.2 M NaCl followed by RNaseA and ProteinaseK treatment. DNA was purified using the Qiagen MinElute kit and used to prepare DNA libraries for sequencing and qPCR validation.

### **Library preparation and sequencing**

DNA libraries were prepared for sequencing as previously described (29). End-repair and A-tailing of DNA fragments were achieved using NEBNext End Repair Enzyme Mix (#E6051A) and 3'-5' exo Klenow fragment (#E6054A). Indexed adaptors (NEXTflex DNA-Seq barcoded adaptors) were ligated (NEB Quick Ligase, #M2200L) to fragments that were then size selected (250 bp) using 0.7x AMPure XP beads (Beckman Coulter). The selected fragments were amplified using KAPA HiFi with dNTPs, and NEXTflex primer mix (#NOVA-514107-96). The PCR products were purified (0.9x AMPure XP beads) and quantified using the Qubit fluorometer HS DNA kit. Sequencing was carried out on an Illumina HiSeq 2500.

**ChIP-qPCR:** ChIP-qPCR was performed on the same material used for ChIP-seq with primers listed in Additional file 4: Table S8. Using serial dilutions of 3D7 genomic DNA all primers were determined to be > 90% efficient and specific, evidenced by single peaks on the melting curves. ChIP-qPCR data were obtained using the Applied Biosystems 7500 Real-Time PCR machine and SDS v1.4 and analysed using the  $\Delta\Delta C_t$  method. Values are expressed as fold enrichment of immunoprecipitated to input DNA, averaged for two biological replicates.

**Detection of changes in histone methylation:** Gametocytes were treated with JIB-04 (5 µM) on days 2, 3 and 4 of development and sampled 24 h later. Histones were extracted as described before (17) with minor modifications. Nuclei were extracted by Dounce homogenisation in hypotonic lysis buffer (10 mM Tris-HCl (pH 8), 0.25 M sucrose, 3 mM MgCl<sub>2</sub>, 0.2% (v/v) Nonidet P-40) and protease inhibitors (Roche)). Histones were isolated from nuclei resuspended in Tris buffer (10 mM Tris (pH 8.0), 0.8 M NaCl, 1 mM EDTA and protease inhibitors) by overnight acid-extraction (0.25 M HCl, with rotation at 4 °C) and subsequent precipitated with 20% TCA. Histone pellets were washed with acetone, reconstituted in dddH<sub>2</sub>O and spotted quantitatively (100 ng per sample) on nitrocellulose membranes. Membranes were submerged in blocking buffer for 30 min followed by 1 h incubation with  $\alpha$ -H3K36me2 (Abcam, ab9049) or  $\alpha$ -H3K36me3 (Abcam, ab9050) primary antibody dilutions (1:5000 in TBS-t). Membranes were washed

three times in TBS-t and then incubated with goat  $\alpha$ -rabbit IgG antibody conjugated to HRP (1:10000) for 1 h. Chemiluminescent signal (Pierce SuperSignal West Pico PLUS Chemiluminescent Substrate) was quantified with ImageJ analysis software (109).

## DNA Microarrays

DNA microarrays (60-mer, Agilent Technologies, USA) based on the full *P. falciparum* genome as previously described (110) were used to assess global transcriptomic changes in gametocytes treated with JIB-04. Day 2 and day 3 gametocyte cultures (1–3% gametocytaemia, 4% haematocrit) were treated with 5  $\mu$ M JIB-04 (Cayman Chemicals) for 24 h followed by isolation of gametocytes using 0.01% (w/v) saponin. Total RNA was isolated with a combination of TRIzol (Sigma Aldrich, USA) and phenol-chloroform extraction and subsequently used to synthesise cDNA as previously described (110) for the untreated and JIB-04 treated day 2 and day 3 gametocyte samples. Sample cDNA was labelled with Cy5 dye (GE Healthcare, USA) prior to hybridisation to arrays with an equal amount (350–500 ng) of Cy3-labelled (GE Healthcare, USA) reference pool containing equal amounts of cDNA from each gametocyte sample and mixed stage 3D7 asexual parasites. After hybridisation, the slides were scanned on a G2600D (Agilent Technologies, USA) scanner and normalised signal intensities for each oligo were extracted using the GE2\_1100\_Jul11\_no\_spikein protocol and Agilent Feature Extractor Software (v 11.5.1.1) as described before (110).

**Data analysis: ChIP-seq:** Sequence read quality was determined using FastQC (111) prior to analysis and adapter sequences were removed using Trimmomatic (v0.32.3) (112). Reads were mapped to the *P. falciparum* 3D7 genome (v39 obtained from PlasmoDB) and duplicate and low-quality reads filtered using BWA-MEM (v0.4.1) (113) and SAMtools (v1.1.2) (114), respectively. Correlation between corresponding biological replicates was determined prior to subsequent analysis. The deepTools suite (v3.1.2.0.0) (115) was used to plot the average enrichment of hPTMs (plotProfile and plotHeatmap tools) and to generate bigwig files containing  $\log_2(\text{ChIP}/\text{input})$  that were viewed in IGV (116). Occupancy of the hPTMs was calculated and are reported as  $\log_2$ -transformed ChIP/input ratios averaged for 1 kb bins. Occupancy 750 bp upstream of gene SS (obtained from PlasmoDB, genome release v39) was calculated from  $\log_2$ ChIP/input ratios over 50 bp bins averaged across the region. All results are representative of data averaged for two biological replicates unless otherwise stated. GO enrichment analyses were performed with PlasmoDB using a *P*-value cut-off  $\leq 0.05$ .

## DNA Microarrays

Normalisation of array data (Robust-spline for within-array and G-quantile for between slide normalisation) was performed in R (v3.2.3, [www.r-project.org](http://www.r-project.org)) using the limma and marray packages. The fit of a linear model was used to obtain  $\log_2$ -transformed expression values ( $\log_2\text{Cy5}/\text{Cy3}$ ). Genes with  $\log_2$ -transformed FC  $\geq 0.5$  in either direction were defined as differentially expressed in the JIB-04 treated gametocytes. Visualisation of differentially expressed genes was performed using TIGR MeV with

functional classification of genes to significantly associated biological processes ( $P$ -values  $\leq 0.05$ ) performed using PlasmoDB (v39, [www.plasmodb.org](http://www.plasmodb.org)).

## Abbreviations

### **ChIP-seq**

Chromatin immunoprecipitation followed by sequencing

### **FC**

Fold change

### **EK**

Ethanolamine kinase

### **GO**

Gene ontology

### **H3K36me2&3**

Histone 3 lysine 36 di- and tri-methylation

### **HAT**

Histone acetyltransferase

### **HDAC**

Histone deacetylase

### **HDM**

Histone demethylase

### **HMT**

Histone methyltransferase

### **HP1**

Heterochromatin protein 1

### **hPTM**

histone post-translational modification

### **JMJC**

Jumonji-C

### **KDM**

Lysine demethylase

### **LSD1**

Lysine-specific demethylase 1

### **lysoPC**

Lysophosphatidylcholine

### **NCC**

Next-cycle conversion

### **PC**

Phosphatidylcholine

### **PMT**

Phosphoethanolamine methyltransferase

**SCC**

Same-cycle conversion

**SS**

Start site

## Declarations

### Ethics approval and consent to participate

The human erythrocytes used in this study were collected from healthy volunteers with due approval from the University of Pretoria Health Sciences Ethics Committee (506/2018).

### Consent for publication

N/A

### Availability of data and materials

The ChIP-seq datasets generated and supporting the conclusions of this article are deposited in the NCBI Sequence Read Archive, accession number GSE163432 available at <https://www.ncbi.nlm.nih.gov/geo/query/acc.cgi?acc=GSE163432>. DNA microarray data are available from the Gene Expression Omnibus repository, accession number GSE163189, <https://www.ncbi.nlm.nih.gov/geo/query/acc.cgi?acc=GSE163189>. Microarray time-course data (34) were obtained from the Gene Expression Omnibus (GEO) under the accession number GSE104889 and presented as expression values ( $\log_2$ Cy5/Cy3) in heatmaps generated using TIGR MeV. Additional data sets pertaining to H3K9me3/HP1 in early gametocytes (GSE102695), AP2-G promoter binding sites (GSE120448), and H3K9me3 in late gametocytes (SRP091939) were obtained from GEO and SRA (27, 29, 33). The panel of commitment- and development-specific genes was compiled from supplementary data files associated with publications with the following DOIs:

<http://dx.doi.org/10.1371/journal.ppat.1000569>, <http://dx.doi.org/10.1016/j.chom.2018.01.008>, <http://dx.doi.org/10.1073/pnas.1217712110>, <http://dx.doi.org/10.1016/j.molbiopara.2005.05.010>, <http://dx.doi.org/10.1126/science.aan6042>, <http://dx.doi.org/10.1371/journal.ppat.1002964>, <http://dx.doi.org/10.1016/j.cell.2017.10.020>, <http://dx.doi.org/10.1038/s41467-020-15026-0>, <http://dx.doi.org/10.1186/s12864-019-6322-9> (25, 27, 29, 34, 42-46). Data pertaining to the transcriptome analysis of JIB-04 in asexual parasites, BIX-01294 and TSA were obtained from the supplementary files associated with the following DOIs: <http://dx.doi.org/10.1021/acsinfecdis.9b00455>, <http://dx.doi.org/10.3390/ijms20205087> and <http://dx.doi.org/10.3389/fcimb.2017.00320>, respectively (38, 71, 72).

### Competing interests

The authors declare no competing interests.

## **Funding**

This work was supported by the South African Medical Department of Science and Innovation and National Research Foundation South African Research Chairs Initiative Grant (LMB UID: 84627).

## **Authors' contributions**

JC conducted the experimental work and data analysis and JR provided technical assistance. GJ and LO provided training and assistance with laboratory experiments. Experiments were conducted in the laboratories of ML and LMB. LMB conceptualised the work and supervised the project. JC and LMB wrote the paper. All authors contributed to and approved the final manuscript.

## **Author information**

### **Affiliations**

**Department of Biochemistry, Genetics and Microbiology, Institute for Sustainable Malaria Control, University of Pretoria, Private bag x20, Hatfield, Pretoria, South Africa**

Jessica Connacher, Janette Reader & Lyn-Marie Birkholtz

**Department of Biochemistry & Molecular Biology and Center for Malaria Research, Pennsylvania State University, University Park, Pennsylvania, 16802, USA.**

Gabrielle Josling, Lindsey Orchard and Manuel Llinás

**Department of Chemistry, Pennsylvania State University, University Park, Pennsylvania, 16802, USA.**

Manuel Llinás

### **Corresponding author**

Correspondence to Lyn-Marie Birkholtz.

## **References**

1. World Health Organization. World malaria report 2020. (2020)
2. Bruce MC, Alano P, Duthie S, Carter R. Commitment of the malaria parasite *Plasmodium falciparum* to sexual and asexual development. *Parasitology*. 1990;100 Pt 2:191-200.
3. Josling GA, Llinas M. Sexual development in *Plasmodium* parasites: knowing when it's time to commit. *Nat Rev Microbiol*. 2015;13(9):573-87.

4. Bancells C, Llorca-Batlle O, Poran A, Notzel C, Rovira-Graells N, Elemento O, et al. Revisiting the initial steps of sexual development in the malaria parasite *Plasmodium falciparum*. *Nat Microbiol*. 2019;4(1):144-54.
5. Josling GA, Williamson KC, Llinas M. Regulation of Sexual Commitment and Gametocytogenesis in Malaria Parasites. *Annu Rev Microbiol*. 2018;72:501-19.
6. Burrows JN, Duparc S, Gutteridge WE, Hooft van Huijsduijnen R, Kaszubska W, Macintyre F, et al. New developments in anti-malarial target candidate and product profiles. *Malar J*. 2017;16(1):26.
7. Cui L, Lindner S, Miao J. Translational regulation during stage transitions in malaria parasites. *Ann N Y Acad Sci*. 2015;1342:1-9.
8. Horrocks P, Wong E, Russell K, Emes RD. Control of gene expression in *Plasmodium falciparum* - ten years on. *Mol Biochem Parasitol*. 2009;164(1):9-25.
9. Llinas M, Deitsch KW, Voss TS. *Plasmodium* gene regulation: far more to factor in. *Trends Parasitol*. 2008;24(12):551-6.
10. Cortes A, Deitsch KW. Malaria Epigenetics. *Cold Spring Harb Perspect Med*. 2017;7(7).
11. Coetzee N, Sidoli S, van Biljon R, Painter H, Llinas M, Garcia BA, et al. Quantitative chromatin proteomics reveals a dynamic histone post-translational modification landscape that defines asexual and sexual *Plasmodium falciparum* parasites. *Sci Rep*. 2017;7(1):607.
12. Duffy MF, Selvarajah SA, Josling GA, Petter M. Epigenetic regulation of the *Plasmodium falciparum* genome. *Brief Funct Genomics*. 2014;13(3):203-16.
13. Bartfai R, Hoeijmakers WA, Salcedo-Amaya AM, Smits AH, Janssen-Megens E, Kaan A, et al. H2A.Z demarcates intergenic regions of the *Plasmodium falciparum* epigenome that are dynamically marked by H3K9ac and H3K4me3. *PLoS Pathog*. 2010;6(12):e1001223.
14. Cui L, Miao J, Furuya T, Li X, Su XZ, Cui L. PfGCN5-mediated histone H3 acetylation plays a key role in gene expression in *Plasmodium falciparum*. *Eukaryot Cell*. 2007;6(7):1219-27.
15. Lopez-Rubio JJ, Gontijo AM, Nunes MC, Issar N, Hernandez Rivas R, Scherf A. 5' flanking region of var genes nucleate histone modification patterns linked to phenotypic inheritance of virulence traits in malaria parasites. *Mol Microbiol*. 2007;66(6):1296-305.
16. Salcedo-Amaya AM, van Driel MA, Alako BT, Trelle MB, van den Elzen AM, Cohen AM, et al. Dynamic histone H3 epigenome marking during the intraerythrocytic cycle of *Plasmodium falciparum*. *Proc Natl Acad Sci U S A*. 2009;106(24):9655-60.
17. Trelle MB, Salcedo-Amaya AM, Cohen AM, Stunnenberg HG, Jensen ON. Global histone analysis by mass spectrometry reveals a high content of acetylated lysine residues in the malaria parasite *Plasmodium falciparum*. *J Proteome Res*. 2009;8(7):3439-50.
18. Karmodiya K, Pradhan SJ, Joshi B, Jangid R, Reddy PC, Galande S. A comprehensive epigenome map of *Plasmodium falciparum* reveals unique mechanisms of transcriptional regulation and identifies H3K36me2 as a global mark of gene suppression. *Epigenetics Chromatin*. 2015;8:32.

19. Venkatesh S, Workman JL. Set2 mediated H3 lysine 36 methylation: regulation of transcription elongation and implications in organismal development. *Wiley Interdiscip Rev Dev Biol.* 2013;2(5):685-700.
20. Cheung V, Chua G, Batada NN, Landry CR, Michnick SW, Hughes TR, et al. Chromatin- and transcription-related factors repress transcription from within coding regions throughout the *Saccharomyces cerevisiae* genome. *PLoS Biol.* 2008;6(11):e277.
21. Strahl BD, Grant PA, Briggs SD, Sun ZW, Bone JR, Caldwell JA, et al. Set2 is a nucleosomal histone H3-selective methyltransferase that mediates transcriptional repression. *Mol Cell Biol.* 2002;22(5):1298-306.
22. Jiang L, Mu J, Zhang Q, Ni T, Srinivasan P, Rayavara K, et al. PfSETvs methylation of histone H3K36 represses virulence genes in *Plasmodium falciparum*. *Nature.* 2013;499(7457):223-7.
23. Lopez-Rubio JJ, Mancio-Silva L, Scherf A. Genome-wide analysis of heterochromatin associates clonally variant gene regulation with perinuclear repressive centers in malaria parasites. *Cell Host Microbe.* 2009;5(2):179-90.
24. Scherf A, Lopez-Rubio JJ, Riviere L. Antigenic variation in *Plasmodium falciparum*. *Annu Rev Microbiol.* 2008;62:445-70.
25. Flueck C, Bartfai R, Volz J, Niederwieser I, Salcedo-Amaya AM, Alako BT, et al. *Plasmodium falciparum* heterochromatin protein 1 marks genomic loci linked to phenotypic variation of exported virulence factors. *PLoS Pathog.* 2009;5(9):e1000569.
26. Brancucci NMB, Bertschi NL, Zhu L, Niederwieser I, Chin WH, Wampfler R, et al. Heterochromatin protein 1 secures survival and transmission of malaria parasites. *Cell Host Microbe.* 2014;16(2):165-76.
27. Fraschka SA, Filarsky M, Hoo R, Niederwieser I, Yam XY, Brancucci NMB, et al. Comparative Heterochromatin Profiling Reveals Conserved and Unique Epigenome Signatures Linked to Adaptation and Development of Malaria Parasites. *Cell Host Microbe.* 2018;23(3):407-20 e8.
28. Kafsack BF, Rovira-Graells N, Clark TG, Bancells C, Crowley VM, Campino SG, et al. A transcriptional switch underlies commitment to sexual development in malaria parasites. *Nature.* 2014;507(7491):248-52.
29. Josling GA, Russell TJ, Venezia J, Orchard L, van Biljon R, Painter HJ, et al. Dissecting the role of PfAP2-G in malaria gametocytogenesis. *Nat Commun.* 2020;11(1):1503.
30. Sinha A, Hughes KR, Modrzynska KK, Otto TD, Pfander C, Dickens NJ, et al. A cascade of DNA-binding proteins for sexual commitment and development in *Plasmodium*. *Nature.* 2014;507(7491):253-7.
31. Bunnik EM, Polishko A, Prudhomme J, Ponts N, Gill SS, Lonardi S, et al. DNA-encoded nucleosome occupancy is associated with transcription levels in the human malaria parasite *Plasmodium falciparum*. *BMC Genomics.* 2014;15:347.
32. Cui L, Miao J. Chromatin-mediated epigenetic regulation in the malaria parasite *Plasmodium falciparum*. *Eukaryot Cell.* 2010;9(8):1138-49.

33. Bunnik EM, Cook KB, Varoquaux N, Batugedara G, Prudhomme J, Cort A, et al. Changes in genome organization of parasite-specific gene families during the Plasmodium transmission stages. *Nat Commun.* 2018;9(1):1910.
34. van Biljon R, van Wyk R, Painter HJ, Orchard L, Reader J, Niemand J, et al. Hierarchical transcriptional control regulates Plasmodium falciparum sexual differentiation. *BMC Genomics.* 2019;20(1):920.
35. Zhu J, Adli M, Zou JY, Verstappen G, Coyne M, Zhang X, et al. Genome-wide chromatin state transitions associated with developmental and environmental cues. *Cell.* 2013;152(3):642-54.
36. Wong MPM, Ng, R. K. Resetting Cell Fate by Epigenetic Reprogramming. In: Logie CaK, T. A., editor. *Chromatin and Epigenetics: IntechOpen; 2020.*
37. Vanheer LN, Zhang H, Lin G, Kafsack BFC. Activity of Epigenetic Inhibitors against Plasmodium falciparum Asexual and Sexual Blood Stages. *Antimicrob Agents Chemother.* 2020;64(7).
38. Matthews KA, Senagbe KM, Notzel C, Gonzales CA, Tong X, Rijo-Ferreira F, et al. Disruption of the Plasmodium falciparum Life Cycle through Transcriptional Reprogramming by Inhibitors of Jumonji Demethylases. *ACS Infect Dis.* 2020;6(5):1058-75.
39. Zhang M, Wang C, Otto TD, Oberstaller J, Liao X, Adapa SR, et al. Uncovering the essential genes of the human malaria parasite Plasmodium falciparum by saturation mutagenesis. *Science.* 2018;360(6388).
40. Bozdech Z, Llinas M, Pulliam BL, Wong ED, Zhu J, DeRisi JL. The transcriptome of the intraerythrocytic developmental cycle of Plasmodium falciparum. *PLoS Biol.* 2003;1(1):E5.
41. Miao J, Fan Q, Cui L, Li J, Li J, Cui L. The malaria parasite Plasmodium falciparum histones: organization, expression, and acetylation. *Gene.* 2006;369:53-65.
42. Brancucci NMB, Gerdt JP, Wang C, De Niz M, Philip N, Adapa SR, et al. Lysophosphatidylcholine Regulates Sexual Stage Differentiation in the Human Malaria Parasite Plasmodium falciparum. *Cell.* 2017;171(7):1532-44 e15.
43. Eksi S, Haile Y, Furuya T, Ma L, Su X, Williamson KC. Identification of a subtelomeric gene family expressed during the asexual-sexual stage transition in Plasmodium falciparum. *Mol Biochem Parasitol.* 2005;143(1):90-9.
44. Eksi S, Morahan BJ, Haile Y, Furuya T, Jiang H, Ali O, et al. Plasmodium falciparum gametocyte development 1 (Pfgdv1) and gametocytogenesis early gene identification and commitment to sexual development. *PLoS Pathog.* 2012;8(10):e1002964.
45. Filarsky M, Fraschka SA, Niederwieser I, Brancucci NMB, Carrington E, Carrio E, et al. GDV1 induces sexual commitment of malaria parasites by antagonizing HP1-dependent gene silencing. *Science.* 2018;359(6381):1259-63.
46. Ikadai H, Shaw Saliba K, Kanzok SM, McLean KJ, Tanaka TQ, Cao J, et al. Transposon mutagenesis identifies genes essential for Plasmodium falciparum gametocytogenesis. *Proc Natl Acad Sci U S A.* 2013;110(18):E1676-84.
47. Hopp CS, Balaban AE, Bushell ES, Billker O, Rayner JC, Sinnis P. Palmitoyl transferases have critical roles in the development of mosquito and liver stages of Plasmodium. *Cell Microbiol.*

- 2016;18(11):1625-41.
48. Santos JM, Duarte N, Kehrer J, Ramesar J, Avramut MC, Koster AJ, et al. Maternally supplied S-acyl-transferase is required for crystalloid organelle formation and transmission of the malaria parasite. *Proc Natl Acad Sci U S A*. 2016;113(26):7183-8.
  49. Tay CL, Jones ML, Hodson N, Theron M, Choudhary JS, Rayner JC. Study of Plasmodium falciparum DHHC palmitoyl transferases identifies a role for PfDHHC9 in gametocytogenesis. *Cell Microbiol*. 2016;18(11):1596-610.
  50. Mancio-Silva L, Lopez-Rubio JJ, Claes A, Scherf A. Sir2a regulates rDNA transcription and multiplication rate in the human malaria parasite Plasmodium falciparum. *Nat Commun*. 2013;4:1530.
  51. Volz J, Carvalho TG, Ralph SA, Gilson P, Thompson J, Tonkin CJ, et al. Potential epigenetic regulatory proteins localise to distinct nuclear sub-compartments in Plasmodium falciparum. *Int J Parasitol*. 2010;40(1):109-21.
  52. Cui L, Fan Q, Cui L, Miao J. Histone lysine methyltransferases and demethylases in Plasmodium falciparum. *Int J Parasitol*. 2008;38(10):1083-97.
  53. Tsukada Y, Fang J, Erdjument-Bromage H, Warren ME, Borchers CH, Tempst P, et al. Histone demethylation by a family of JmjC domain-containing proteins. *Nature*. 2006;439(7078):811-6.
  54. Whetstine JR, Nottke A, Lan F, Huarte M, Smolikov S, Chen Z, et al. Reversal of histone lysine trimethylation by the JMJD2 family of histone demethylases. *Cell*. 2006;125(3):467-81.
  55. Chen Z, Zang J, Whetstine J, Hong X, Davrazou F, Kutateladze TG, et al. Structural insights into histone demethylation by JMJD2 family members. *Cell*. 2006;125(4):691-702.
  56. Modrzynska K, Pfander C, Chappell L, Yu L, Suarez C, Dundas K, et al. A Knockout Screen of ApiAP2 Genes Reveals Networks of Interacting Transcriptional Regulators Controlling the Plasmodium Life Cycle. *Cell Host Microbe*. 2017;21(1):11-22.
  57. Kent RS, Modrzynska KK, Cameron R, Philip N, Billker O, Waters AP. Inducible developmental reprogramming redefines commitment to sexual development in the malaria parasite Plasmodium berghei. *Nat Microbiol*. 2018;3(11):1206-13.
  58. Llorca-Batlle O, Michel-Todo L, Witmer K, Toda H, Fernandez-Becerra C, Baum J, et al. Conditional expression of PfAP2-G for controlled massive sexual conversion in Plasmodium falciparum. *Sci Adv*. 2020;6(24):eaaz5057.
  59. Singh S, Santos JM, Orchard LM, Yamada N, van Biljon R, Painter HJ, et al. The PfAP2-G2 transcription factor is a critical regulator of gametocyte maturation. *bioRxiv*. 2020:2020.10.27.355685.
  60. Lopez-Rubio JJ, Siegel TN, Scherf A. Genome-wide chromatin immunoprecipitation-sequencing in Plasmodium. *Methods Mol Biol*. 2013;923:321-33.
  61. Perez-Toledo K, Rojas-Meza AP, Mancio-Silva L, Hernandez-Cuevas NA, Delgadillo DM, Vargas M, et al. Plasmodium falciparum heterochromatin protein 1 binds to tri-methylated histone 3 lysine 9 and is linked to mutually exclusive expression of var genes. *Nucleic Acids Res*. 2009;37(8):2596-606.

62. Morahan BJ, Strobel C, Hasan U, Czesny B, Mantel PY, Marti M, et al. Functional analysis of the exported type IV HSP40 protein PfGECO in *Plasmodium falciparum* gametocytes. *Eukaryot Cell*. 2011;10(11):1492-503.
63. Silvestrini F, Lasonder E, Olivieri A, Camarda G, van Schaijk B, Sanchez M, et al. Protein export marks the early phase of gametocytogenesis of the human malaria parasite *Plasmodium falciparum*. *Mol Cell Proteomics*. 2010;9(7):1437-48.
64. Ukaegbu UE, Kishore SP, Kwiatkowski DL, Pandarinath C, Dahan-Pasternak N, Dzikowski R, et al. Recruitment of PfSET2 by RNA polymerase II to variant antigen encoding loci contributes to antigenic variation in *P. falciparum*. *PLoS Pathog*. 2014;10(1):e1003854.
65. Coetzee N, von Gruning H, Opperman D, van der Watt M, Reader J, Birkholtz LM. Epigenetic inhibitors target multiple stages of *Plasmodium falciparum* parasites. *Sci Rep*. 2020;10(1):2355.
66. Reader J, Van der Watt ME, Taylor D, Le Manach C, Mittal N, Otilie S, et al. Multistage and transmission-blocking targeted antimalarials discovered from the open-source MMV Pandemic Response Box. *BioRxiv*. 2020.
67. Sengoku T, Yokoyama S. Structural basis for histone H3 Lys 27 demethylation by UTX/KDM6A. *Genes Dev*. 2011;25(21):2266-77.
68. Tiburcio M, Silvestrini F, Bertuccini L, Sander AF, Turner L, Lavstsen T, et al. Early gametocytes of the malaria parasite *Plasmodium falciparum* specifically remodel the adhesive properties of infected erythrocyte surface. *Cell Microbiol*. 2013;15(4):647-59.
69. Volz JC, Bartfai R, Petter M, Langer C, Josling GA, Tsuboi T, et al. PfSET10, a *Plasmodium falciparum* methyltransferase, maintains the active var gene in a poised state during parasite division. *Cell Host Microbe*. 2012;11(1):7-18.
70. Santos JM, Josling G, Ross P, Joshi P, Orchard L, Campbell T, et al. Red Blood Cell Invasion by the Malaria Parasite Is Coordinated by the PfAP2-I Transcription Factor. *Cell Host Microbe*. 2017;21(6):731-41 e10.
71. Ngwa CJ, Kiesow MJ, Orchard LM, Farrukh A, Llinas M, Pradel G. The G9a Histone Methyltransferase Inhibitor BIX-01294 Modulates Gene Expression during *Plasmodium falciparum* Gametocyte Development and Transmission. *Int J Mol Sci*. 2019;20(20).
72. Ngwa CJ, Kiesow MJ, Papst O, Orchard LM, Filarsky M, Rosinski AN, et al. Transcriptional Profiling Defines Histone Acetylation as a Regulator of Gene Expression during Human-to-Mosquito Transmission of the Malaria Parasite *Plasmodium falciparum*. *Front Cell Infect Microbiol*. 2017;7:320.
73. Wang L, Chang J, Varghese D, Dellinger M, Kumar S, Best AM, et al. A small molecule modulates Jumonji histone demethylase activity and selectively inhibits cancer growth. *Nat Commun*. 2013;4:2035.
74. Delves MJ. *Plasmodium* cell biology should inform strategies used in the development of antimalarial transmission-blocking drugs. *Future Med Chem*. 2012;4(18):2251-63.

75. Issar N, Ralph SA, Mancio-Silva L, Keeling C, Scherf A. Differential sub-nuclear localisation of repressive and activating histone methyl modifications in *P. falciparum*. *Microbes Infect.* 2009;11(3):403-7.
76. Yuan S, Natesan R, Sanchez-Rivera FJ, Li J, Bhanu NV, Yamazoe T, et al. Global Regulation of the Histone Mark H3K36me2 Underlies Epithelial Plasticity and Metastatic Progression. *Cancer Discov.* 2020;10(6):854-71.
77. Suzuki S, Kato H, Suzuki Y, Chikashige Y, Hiraoka Y, Kimura H, et al. Histone H3K36 trimethylation is essential for multiple silencing mechanisms in fission yeast. *Nucleic Acids Res.* 2016;44(9):4147-62.
78. Chantalat S, Depaux A, Hery P, Barral S, Thuret JY, Dimitrov S, et al. Histone H3 trimethylation at lysine 36 is associated with constitutive and facultative heterochromatin. *Genome Res.* 2011;21(9):1426-37.
79. Kuo AJ, Cheung P, Chen K, Zee BM, Kioi M, Lauring J, et al. NSD2 links dimethylation of histone H3 at lysine 36 to oncogenic programming. *Mol Cell.* 2011;44(4):609-20.
80. Pokholok DK, Harbison CT, Levine S, Cole M, Hannett NM, Lee TI, et al. Genome-wide map of nucleosome acetylation and methylation in yeast. *Cell.* 2005;122(4):517-27.
81. Rao B, Shibata Y, Strahl BD, Lieb JD. Dimethylation of histone H3 at lysine 36 demarcates regulatory and nonregulatory chromatin genome-wide. *Mol Cell Biol.* 2005;25(21):9447-59.
82. Sinha I, Buchanan L, Ronnerblad M, Bonilla C, Durand-Dubief M, Shevchenko A, et al. Genome-wide mapping of histone modifications and mass spectrometry reveal H4 acetylation bias and H3K36 methylation at gene promoters in fission yeast. *Epigenomics.* 2010;2(3):377-93.
83. Woo H, Dam Ha S, Lee SB, Buratowski S, Kim T. Modulation of gene expression dynamics by co-transcriptional histone methylations. *Exp Mol Med.* 2017;49(4):e326.
84. Wu SF, Zhang H, Cairns BR. Genes for embryo development are packaged in blocks of multivalent chromatin in zebrafish sperm. *Genome Res.* 2011;21(4):578-89.
85. Huang C, Zhu B. Roles of H3K36-specific histone methyltransferases in transcription: antagonizing silencing and safeguarding transcription fidelity. *Biophys Rep.* 2018;4(4):170-7.
86. Wagner EJ, Carpenter PB. Understanding the language of Lys36 methylation at histone H3. *Nat Rev Mol Cell Biol.* 2012;13(2):115-26.
87. Carrozza MJ, Li B, Florens L, Suganuma T, Swanson SK, Lee KK, et al. Histone H3 methylation by Set2 directs deacetylation of coding regions by Rpd3S to suppress spurious intragenic transcription. *Cell.* 2005;123(4):581-92.
88. Coleman BI, Skillman KM, Jiang RHY, Childs LM, Altenhofen LM, Ganter M, et al. A *Plasmodium falciparum* histone deacetylase regulates antigenic variation and gametocyte conversion. *Cell Host Microbe.* 2014;16(2):177-86.
89. Poran A, Notzel C, Aly O, Mencia-Trinchant N, Harris CT, Guzman ML, et al. Single-cell RNA sequencing reveals a signature of sexual commitment in malaria parasites. *Nature.* 2017;551(7678):95-9.

90. Berr A, McCallum EJ, Menard R, Meyer D, Fuchs J, Dong A, et al. Arabidopsis SET DOMAIN GROUP2 is required for H3K4 trimethylation and is crucial for both sporophyte and gametophyte development. *Plant Cell*. 2010;22(10):3232-48.
91. Lee K, Park OS, Jung SJ, Seo PJ. Histone deacetylation-mediated cellular dedifferentiation in Arabidopsis. *J Plant Physiol*. 2016;191:95-100.
92. He C, Chen X, Huang H, Xu L. Reprogramming of H3K27me3 is critical for acquisition of pluripotency from cultured Arabidopsis tissues. *PLoS Genet*. 2012;8(8):e1002911.
93. Janse CJ, Ponnudurai T, Lensen AH, Meuwissen JH, Ramesar J, Van der Ploeg M, et al. DNA synthesis in gametocytes of Plasmodium falciparum. *Parasitology*. 1988;96 ( Pt 1):1-7.
94. Sinden RE, Canning EU, Bray RS, Smalley ME. Gametocyte and gamete development in Plasmodium falciparum. *Proc R Soc Lond B Biol Sci*. 1978;201(1145):375-99.
95. Joice R, Nilsson SK, Montgomery J, Dankwa S, Egan E, Morahan B, et al. Plasmodium falciparum transmission stages accumulate in the human bone marrow. *Sci Transl Med*. 2014;6(244):244re5.
96. Pelle KG, Oh K, Buchholz K, Narasimhan V, Joice R, Milner DA, et al. Transcriptional profiling defines dynamics of parasite tissue sequestration during malaria infection. *Genome Med*. 2015;7(1):19.
97. Tiburcio M, Sauerwein R, Lavazec C, Alano P. Erythrocyte remodeling by Plasmodium falciparum gametocytes in the human host interplay. *Trends Parasitol*. 2015;31(6):270-8.
98. Alano P. Plasmodium falciparum gametocytes: still many secrets of a hidden life. *Mol Microbiol*. 2007;66(2):291-302.
99. Dhayalan A, Rajavelu A, Rathert P, Tamas R, Jurkowska RZ, Ragozin S, et al. The Dnmt3a PWWP domain reads histone 3 lysine 36 trimethylation and guides DNA methylation. *J Biol Chem*. 2010;285(34):26114-20.
100. Chen ES, Zhang K, Nicolas E, Cam HP, Zofall M, Grewal SI. Cell cycle control of centromeric repeat transcription and heterochromatin assembly. *Nature*. 2008;451(7179):734-7.
101. Lu Q, Qiu X, Hu N, Wen H, Su Y, Richardson BC. Epigenetics, disease, and therapeutic interventions. *Ageing Res Rev*. 2006;5(4):449-67.
102. Hoeijmakers WA, Stunnenberg HG, Bartfai R. Placing the Plasmodium falciparum epigenome on the map. *Trends Parasitol*. 2012;28(11):486-95.
103. Birkholtz L, van Brummelen AC, Clark K, Niemand J, Marechal E, Llinas M, et al. Exploring functional genomics for drug target and therapeutics discovery in Plasmodia. *Acta Trop*. 2008;105(2):113-23.
104. Trager W, Jensen JB. Human malaria parasites in continuous culture. *Science*. 1976;193(4254):673-5.
105. Lambros C, Vanderberg JP. Synchronization of Plasmodium falciparum erythrocytic stages in culture. *J Parasitol*. 1979;65(3):418-20.
106. Carter R, Ranford-Cartwright L, Alano P. The culture and preparation of gametocytes of Plasmodium falciparum for immunochemical, molecular, and mosquito infectivity studies. *Methods Mol Biol*. 1993;21:67-88.

107. Reader J, Botha M, Theron A, Lauterbach SB, Rossouw C, Engelbrecht D, et al. Nowhere to hide: interrogating different metabolic parameters of Plasmodium falciparum gametocytes in a transmission blocking drug discovery pipeline towards malaria elimination. *Malar J.* 2015;14:213.
108. van Biljon R, Niemand J, van Wyk R, Clark K, Verlinden B, Abrie C, et al. Inducing controlled cell cycle arrest and re-entry during asexual proliferation of Plasmodium falciparum malaria parasites. *Sci Rep.* 2018;8(1):16581.
109. Schneider CA, Rasband WS, Eliceiri KW. NIH Image to ImageJ: 25 years of image analysis. *Nat Methods.* 2012;9(7):671-5.
110. Painter HJ, Altenhofen LM, Kafsack BF, Llinas M. Whole-genome analysis of Plasmodium spp. Utilizing a new agilent technologies DNA microarray platform. *Methods Mol Biol.* 2013;923:213-9.
111. Andrews S. FastQC: a quality control tool for high throughput sequence data 2010 [cited 2019]. Available from: <http://www.bioinformatics.babraham.ac.uk/projects/fastqc>.
112. Bolger AM, Lohse M, Usadel B. Trimmomatic: a flexible trimmer for Illumina sequence data. *Bioinformatics.* 2014;30(15):2114-20.
113. Li H, Durbin R. Fast and accurate long-read alignment with Burrows-Wheeler transform. *Bioinformatics.* 2010;26(5):589-95.
114. Li H, Handsaker B, Wysoker A, Fennell T, Ruan J, Homer N, et al. The Sequence Alignment/Map format and SAMtools. *Bioinformatics.* 2009;25(16):2078-9.
115. Ramirez F, Dundar F, Diehl S, Gruning BA, Manke T. deepTools: a flexible platform for exploring deep-sequencing data. *Nucleic Acids Res.* 2014;42(Web Server issue):W187-91.
116. Thorvaldsdottir H, Robinson JT, Mesirov JP. Integrative Genomics Viewer (IGV): high-performance genomics data visualization and exploration. *Brief Bioinform.* 2013;14(2):178-92.

## Figures

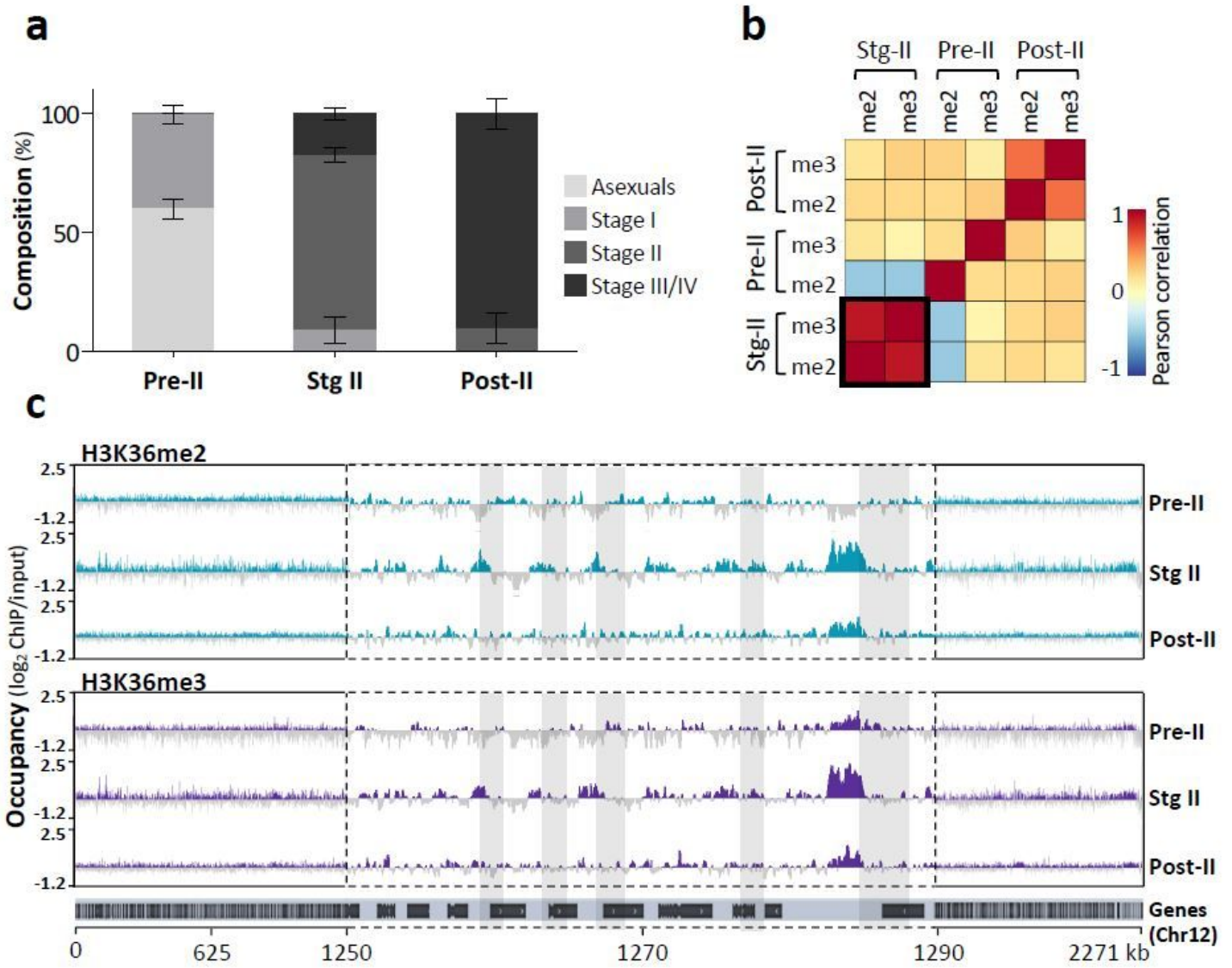


**Figure 1**

Our ChIP-seq results show that unique patterns of H3K36me2&3 occupancy occur at each of the gametocyte stages and that both hPTMs are differentially enriched in the stage II gametocytes (Fig. 1).

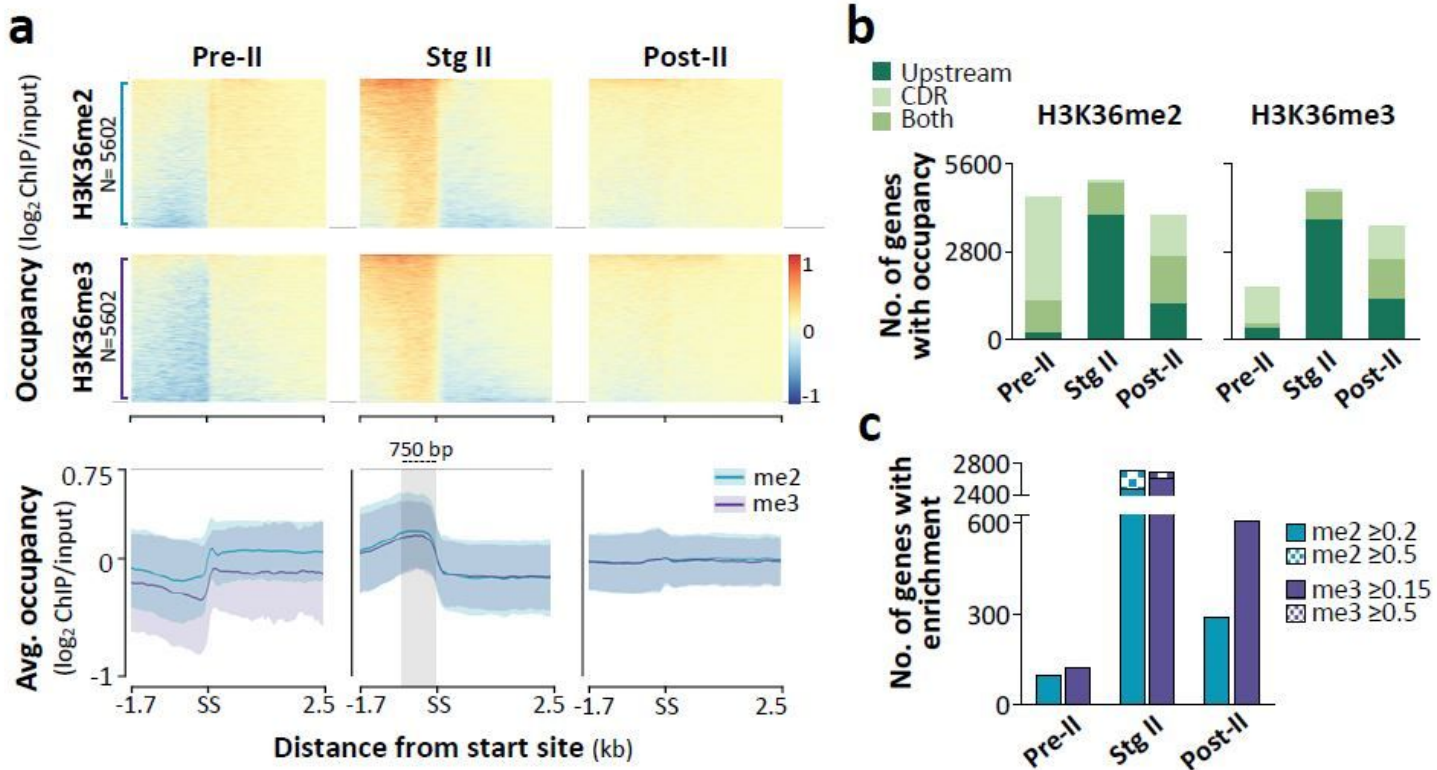


**Figure 2**

The occupancy profiles of H3K36me2&3 are distinctly uniform across the intergenic non-coding regions in stage II gametocytes, contrasting with more variable patterns in the pre- and post-stage II gametocytes (Fig. 2).

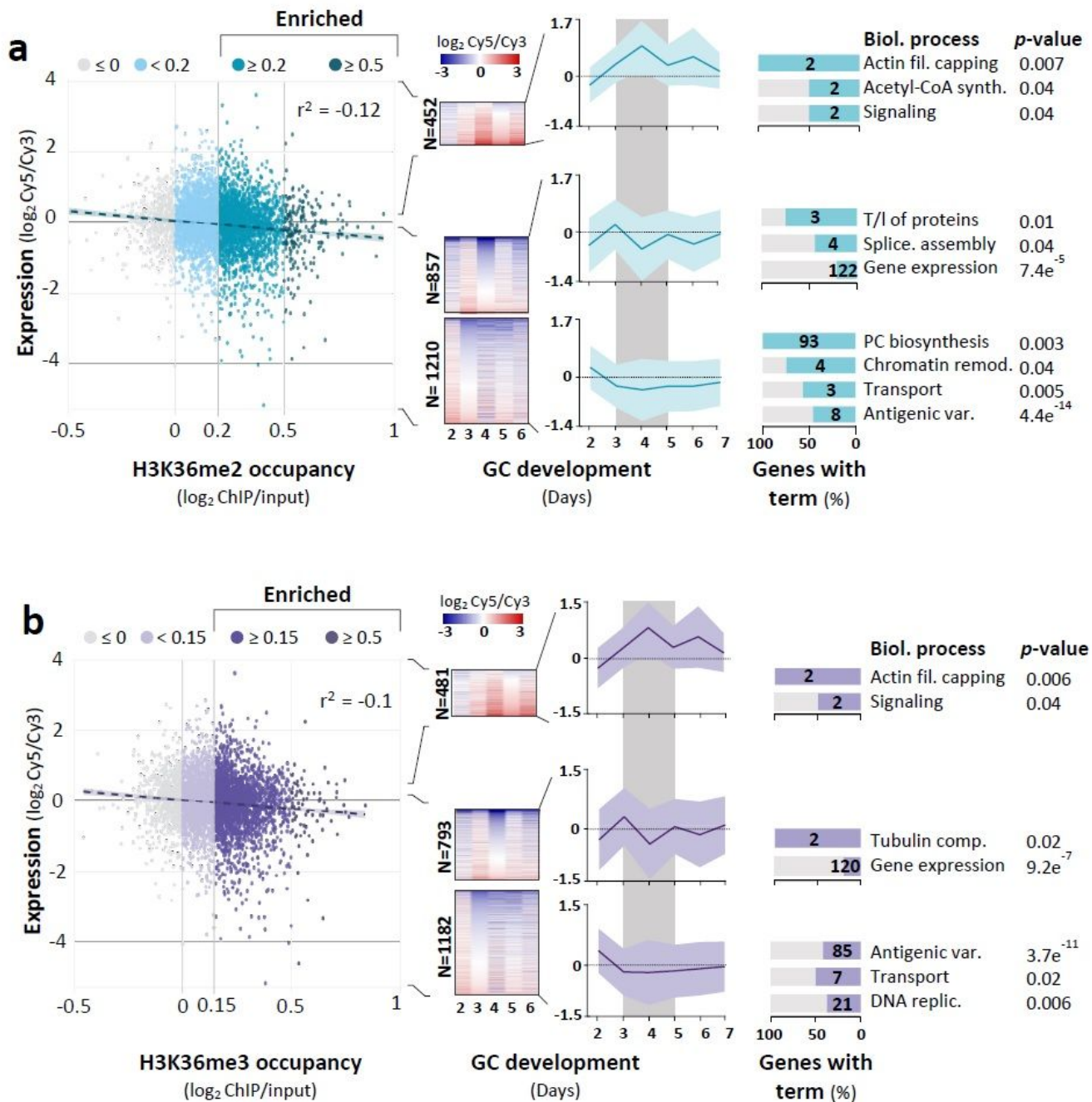


**Figure 3**

The global analysis of the hPTMs upstream of genes and the transcript levels in stage II gametocytes (average  $\log_2 \text{Cy5/Cy3}$  on days 4 and 5 of development associated with stage II gametocytes) indicated that the degree of H3K36me2&3 occupancy is not correlated with the expression (Pearson correlations,  $r^2 = -0.12$  and  $r^2 = -0.1$  for H3K36me2&3, respectively, Fig. 3).

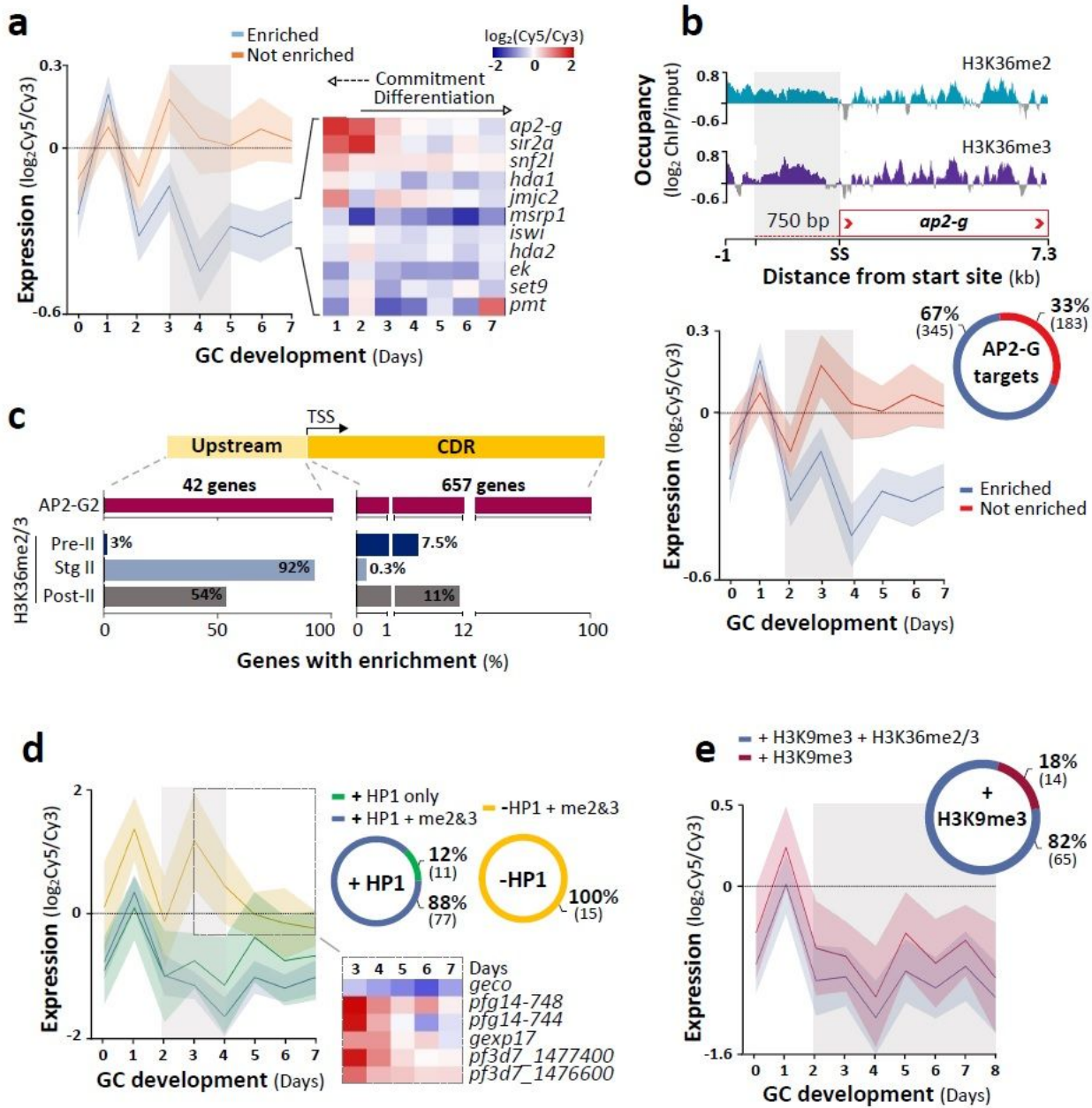


**Figure 4**

Importantly, all the enriched genes have dramatically reduced transcript abundance levels during early gametocyte development compared to those without H3K36me2&3 (average of 6-fold and  $\leq 12$ -fold lower on days 3-7, Fig. 4).

## Supplementary Files

This is a list of supplementary files associated with this preprint. Click to download.

- [Additionalfile2TablesS1S5.xlsx](#)
- [Additionalfile3TableS6.xlsx](#)
- [Additionalfile4TablesS7andS8.xlsx](#)
- [FINALAdditionalfile1FiguresS1S6.pdf](#)